JOURNAL OF MATERIALS SCIENCE 25 (1990) 2771–2776

1300 K compressive properties of several dispersion strengthened NiAl materials

J. DANIEL WHITTENBERGER, D. J. GAYDOSH,
NASA Lewis Research Center, Cleveland, Ohio 44135, USA

K. S. KUMAR
Martin Marietta Laboratories, Baltimore, Maryland 21227-3898, USA

Recently an attempt [8] to produce dispersion hardened NiAl by rapid solidification technology (RST) was discussed; however these microstructural studies and tensile testing procedures did not yield conclusive evidence of strengthening. To examine the potential of RST as a means to fabricate dispersion strengthened aluminides, cylindrical compression samples were machined from the gauge section of their tensile specimens and tested in air at 1300 K: in addition, considerable materialography, including light optical, scanning electron and transmission electron microscopy techniques, of the as-fabricated and compression tested materials was conducted. While microscopy indicates that RST can produce fine dispersions of TiB_2, TiC and HfC in a NiAl matrix, the mechanical property data reveal that only HfC successfully strengthens the intermetallic matrix. The high stress exponents (> 10) and/or independence of strain rate on stress for NiAl–HfC materials suggest elevated temperature mechanical behaviour similar to that found in oxide dispersion strengthened alloys. Furthermore an apparent example of "departure side" pinning has been observed, and as such, it is indicative of a threshold stress for creep.

1. Introduction

While the B2 cubic crystal structure intermetallic phase NiAl is of interest for high temperature structural applications because of its relatively low density and excellent oxidation resistance, it lacks mechanical strength at elevated temperatures [1]. Several approaches are currently being investigated to remedy this situation; these include precipitation of a second phase [2, 3], particulate composites [4, 5] and unidirectional fibre reinforcement [6]. In addition recent work [7, 8] has been reported on a dispersion strengthening approach utilizing rapid solidification technology (RST) to incorporate the hardening phase. Unfortunately the tensile test method, chosen by Jha *et al.* [7, 8] to evaluate the mechanical properties of the dispersion strengthened materials, did not yield conclusive evidence as many test specimens possessed cracks and flaws which induced premature failure. Furthermore attempts [7] to conduct transmission electron microscopy (TEM) analysis to assess the capability of RST to produce a dispersion of particles were unsuccessful.

The current study was instituted to determine more clearly whether NiAl could be successfully dispersion strengthened at elevated temperature by RST. To this end short, cylindrical samples were cut from the untested and/or prematurely failed room temperature and 1033 K tensile test specimens utilized by Jha *et al.* [7, 8] and were then compression tested at 1300 K. This effort utilized all ten compositions fabricated in their original work [7] and included considerable microstructural analysis involving light optical, scanning electron and transmission electron microscopy of as-received and tested materials.

2. Experimental procedures

At our request tested and untested tensile specimens machined from dispersion strengthened NiAl materials were sent by Marko Materials, Inc. to the Lewis Research Center where short, ~ 12 mm, lengths were electro-discharge machined from the nominally 6 mm diameter gauge sections. Such specimens were compression tested at crosshead speeds ranging from 2.12×10^{-3} to 2.12×10^{-6} mm sec^{-1} in air at 1300 K in a universal test machine to ~ 8% strain. The autographically recorded load–time charts were converted to true compressive stresses, strains, and strain rates via the offset method [9, 10] and the assumption of conservation of volume. Microstructural characterization of both as-fabricated and compression tested materials was conducted on selected specimens using light optical, scanning electron (SEM) and transmission electron microscopy techniques.

Sections for TEM examination were taken perpendicular to the compression axis by cutting slices approximately 0.5 mm thick with a high speed diamond saw. These were ground on resin-bonded diamond wheels to a thickness of ~ 0.2 mm, adhesively mounted between glass slides and 3 mm diameter circular discs cut by ultrasonic grinding in a SiC slurry. The discs were electrolytically thinned to perforation with a 10% perchloric–methanol solution at 238 K and 10 to 12 V. If sufficient transparent area was not

0022–2461/90 $03.00 + .12

TABLE I Composition and grain size of dispersion strengthened NiAl

Intended composition (wt %)	Measured composition (at %)	Grain size (μm)		
		As-extruded	After testing 1300 K, $\dot{\varepsilon} \sim 2 \times 10^{-5}$ sec^{-1}	
			Small diameter region	Large grain region*
0.25 TiB_2		2.4	3.9	70 × 400*
1.0 TiB_2		1.3	1.7	
1.5 TiB_2	48.6Al–48. 7Ni–0.9Ti–1.6B–0.12C (~ 1.2 wt % TiB_2)	1.3	1.7	
2.0 TiB_2	48.7Al–47.5Ni–1.1Ti–2.4B–0.15C (~ 1.9 wt % TiB_2)	1.3	2.1	
0.5 HfC		3.7	–	36
1.0 HfC	49.3Al–50.2Ni–0.15Hf–0.31C (~ 0.65 wt % HfC)	1.8	2.0	100 × 540*
2.0 HfC		2.3	2.2	
4.3 HfC		3.3	2.5	345 × 540*
0.25 TiB_2 + 0.5 HfC		2.1	–	65 × 150
2 TiC		2.4	2.2	95 × 130*

*Approximate size of the grains within the regions which have undergone secondary grain growth or recrystallization during testing; long dimension parallel to the extrusion (testing) direction.

present after chemical thinning, the foils were processed further by ion-milling for short periods of time.

3. Results

3.1. Starting materials

Ten equiatomic NiAl alloys (Table I) containing various amounts of HfC, TiB_2 and/or TiC as dispersoids were produced by Marko Materials, Inc. via rapid solidification technology. With the assumption that small additions of HfC, TiB_2 and TiC would be soluble in molten NiAl but not in the solid state, the materials were melted on a cold hearth utilizing a non-consumable tungsten arc and rapidly solidified by melt dragging thin filaments on a rotating molybdenum wheel. Following casting, the threads were shattered in a hammer mill into −40 to +80 mesh particles. Such powders were sealed in evacuated steel cans and hot extruded at a 16 to 1 reduction ratio at 1395 K. Additional details on manufacturing processes can be found in references [7, 8].

Spot checking of several alloys indicated that the actual compositions (Table I) were close to the intended values in terms of Ni to Al ratio and TiB_2 additions; however all examined alloys contained excess carbon. In addition analysis of one HfC containing material revealed that the actual HfC content was about half the expected value.

Light optical and scanning electron microstructural studies of the as-extruded materials showed that the grain sizes were of the order of 2 μm (Table I). Irrespective of the overall composition, high magnification SEM examination of the materials under back scattered electron conditions showed that the HfC, TiB_2 and TiC additions were dispersed as small particles O (30 nm) within the NiAl matrix (Fig. 1a). However, large precipitates which were strung out in the extrusion direction (Fig. 1b) were also observed in the aluminides containing either $2TiB_2$, 2TiC or more than 0.5% HfC. Transmission electron microscopy (Fig. 2) of the $2TiB_2$ and 2HfC aluminides revealed that both these types of particles were located on grain boundaries as well as within the NiAl matrix. In

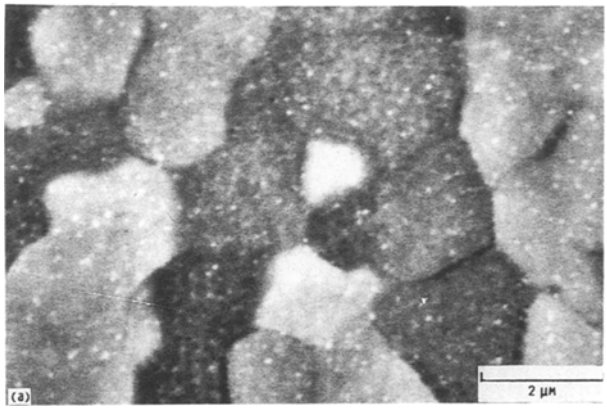

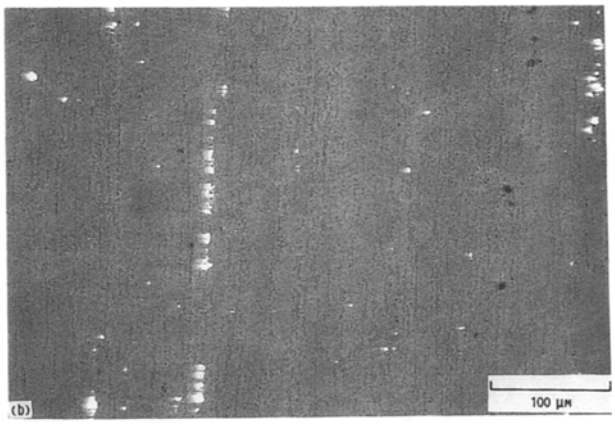

Figure 1 Typical SEM microstructure of as extruded NiAl–2 HfC. (a) dispersed, small HfC particles within NiAl grains and (b) large HfC (white) precipitates aligned along the extrusion axis. Specimens etched with a mixture of 33 HNO_3, 33 acetic acid, 33 H_2O, and 1 HF (parts by volume).

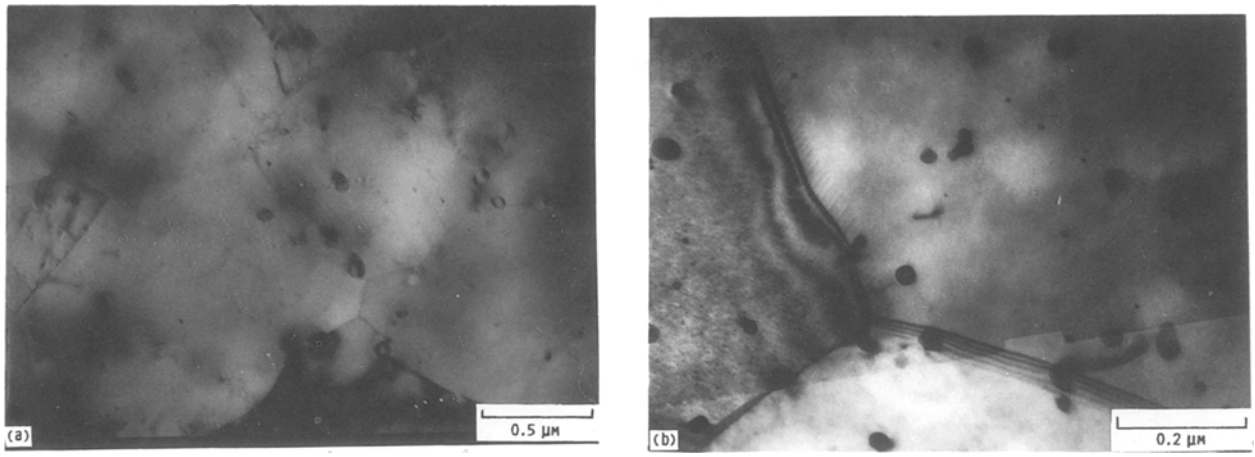

Figure 2 TEM microstructures of as extruded (a) NiAl–2 TiB_2 and (b) NiAl–2 HfC.

addition examples of the particles pinning subgrain boundaries and isolated dislocations were seen in both materials. Although extensive studies were not undertaken it appeared that the average size of the HfC particles (Fig. 2b) was smaller than that for TiB_2 (Fig. 2a), and that the density of particles was greater for the NiAl-2HfC alloy.

3.2. Compression testing

True stress–true strain diagrams for NiAl–TiB_2 and NiAl–HfC materials tested at 1300 K and a nominal strain rate of 2×10^{-6} sec^{-1} are presented in Fig. 3. While both types of material have similar behaviour (either minor work hardening or continuous flow under a constant stress after a few per cent strain), clearly there are large differences in strength between the HfC- and TiB_2-containing aluminides. In addition to demonstrating inconsistent behaviour with respect to amount of dispersoid, the NiAl-TiB_2 materials are no stronger than a 5 μm grain size, binary NiAl* (Fig. 3b). The NiAl–HfC intermetallics, on the other hand, are considerably stronger than NiAl and possess a more reasonable behaviour where strength basically increases with HfC content (Fig. 3b). While resistance to deformation seems to be dependent on HfC level, in reality the strength of the three materials which have between 1 and 4.3 wt % dispersoid is quite similar.

The 1300 K true stress–strain rate behaviour for all ten RST dispersion strengthened NiAl materials is shown in Fig. 4 where the data for these alloys were taken at 5% strain. Again the differences in properties between the HfC and TiB_2 strengthened aluminides are clear; in fact the deformation resistance of NiAl–TiB_2 (Fig. 4a) is less than that for 5 μm NiAl (Fig. 4b). The inconsistency with respect to TiB_2 content, previously noted in Fig. 3a, is evident in the stress–strain rate data; in addition the three points for NiAl–0.25 TiB_2 show considerable scatter. Fig. 4a also demonstrates that the TiC incorporated into NiAl by RST is not an effective dispersion strengthening agent.

Although the materials with lower levels of HfC (i.e. 0.25 TiB_2 + 0.5 HfC, 0.5 HfC and 1 HfC) show normal behaviour where strength decreases with decreasing strain rate (Fig. 4b), the NiAl–2 HfC and NiAl–4.3 HfC did not follow this trend. For these materials

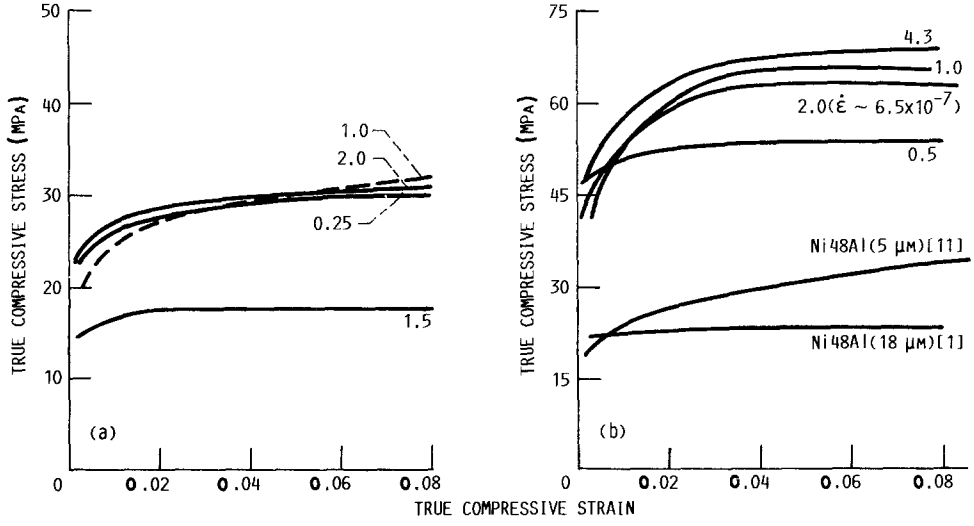

Figure 3 True compressive stress–strain curves for (a) NiAl–TiB_2 and (b) NiAl–HfC intermetallics tested at 1300 K and an approximate strain rate of 2×10^{-6} sec^{-1}.

*The actual composition of binary aluminide labelled Ni 48 Al is Ni–48.25 Al (at. %). The difference in chemistry between this alloy and the nominally 50 Al level in the dispersion strengthen materials has no affect on 1300 K elevated temperature strength [1].

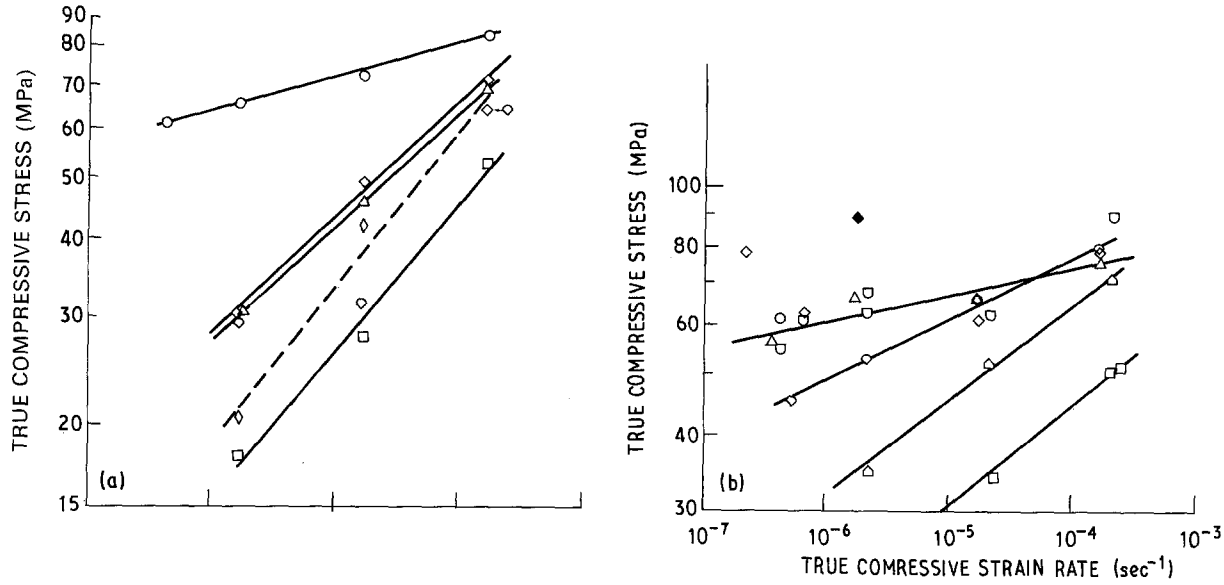

Figure 4 True compressive stress–strain rate behaviour at 1300 K for (a) NiAl–TiB_2 and NiAl–2 TiC and (b) NiAl–HfC intermetallics. Stress and strain rate data taken at 5% strain except for full symbol which represents values at 7% strain.

		(a)			(b)	
		n	R_d^2		n	R_d^2
◊	$0.25TiB_2$	4.7	0.81	0.5HfC	10.1	0.99
○	$0.25TiB_2+0.5HfC$	18.5	0.99			
△	$1.0TiB_2$	5.6	1.00	1.0HfC	22.4	0.90
□	$1.5TiB_2$	4.2	0.98	NiAl(18μm)[1]	5.7	0.99
◇	$2.0TiB_2$	5.3	0.99	2.0HfC	2.0	0.008
◊	2.0TiC	3.9	0.98	4.3HfC	12.0	0.73
⬠				NiAl(5μm)[12]	6.3	0.99

the strength at lower strain rates equalled or even exceeded that measured at fast testing conditions. While seemingly unpredictable in terms of exact strength, the data in Fig. 4b for NiAl–2 HfC and NiAl–4.3 HfC reveal that they are significantly stronger than binary NiAl.

For completeness the data in Fig. 4 were fitted by linear regression techniques to the power law equation

$$\dot{\varepsilon} = A_\sigma^n$$

where $\dot{\varepsilon}$ is the strain rate, σ the flow stress at 5% strain, A a constant and n the stress exponent. Results in terms of the stress exponent, coefficient of determination R_d^2 and, in most cases, the predicted curves are shown for each composition in Fig. 4.

3.3. Post test microstructure

Light optical and SEM examination of the materials tested at 1300 K and a nominal strain rate of 2×10^{-5} sec^{-1} revealed that the initial grain structure was unstable in six of the ten alloys (Table I). Almost complete recrystallization occurred in NiAl–0.25 TiB_2–0.5 HfC and NiAl–0.5 HfC (Fig 5a), while the 0.25 TiB_2-, 1 HfC-, 2 TiC- and, surprisingly,

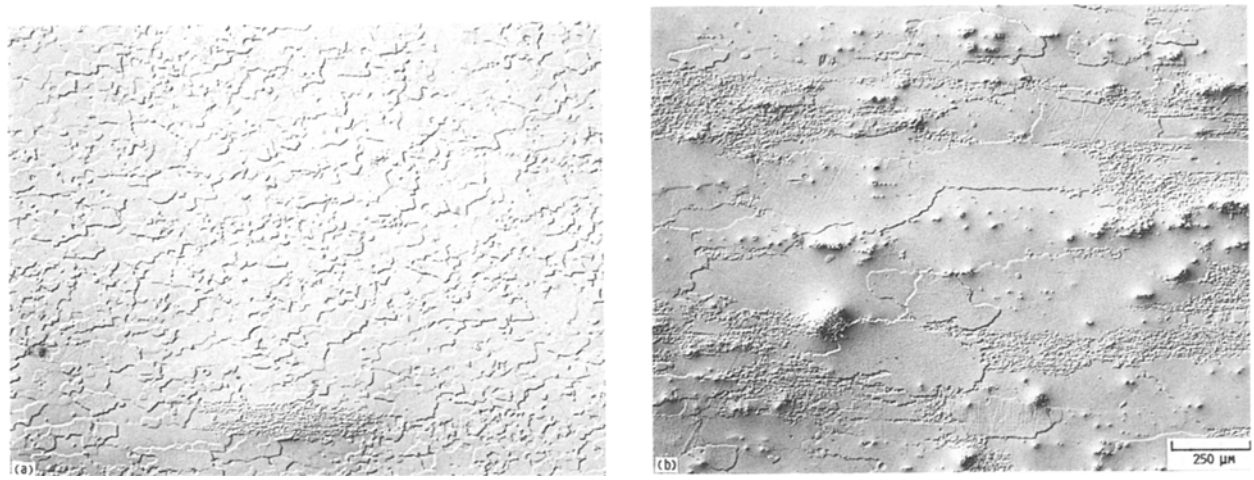

Figure 5 Examples of recrystallization found in specimens tested at 1300 K and a strain rate $\approx 2 \times 10^{-5}$ sec^{-1} to ~ 10 strain: (a) NiAl–0.5 HfC and (b) NiAl–4.3 HfC. Compression axis is horizontal; specimens etched with a mixture of 33 HNO_3, 33 acetic acid, 33 H_2O, and 1 HF (vol %). Photomicrographs taken under differential interference conditions; disruptions in part (b) are large HfC particles.

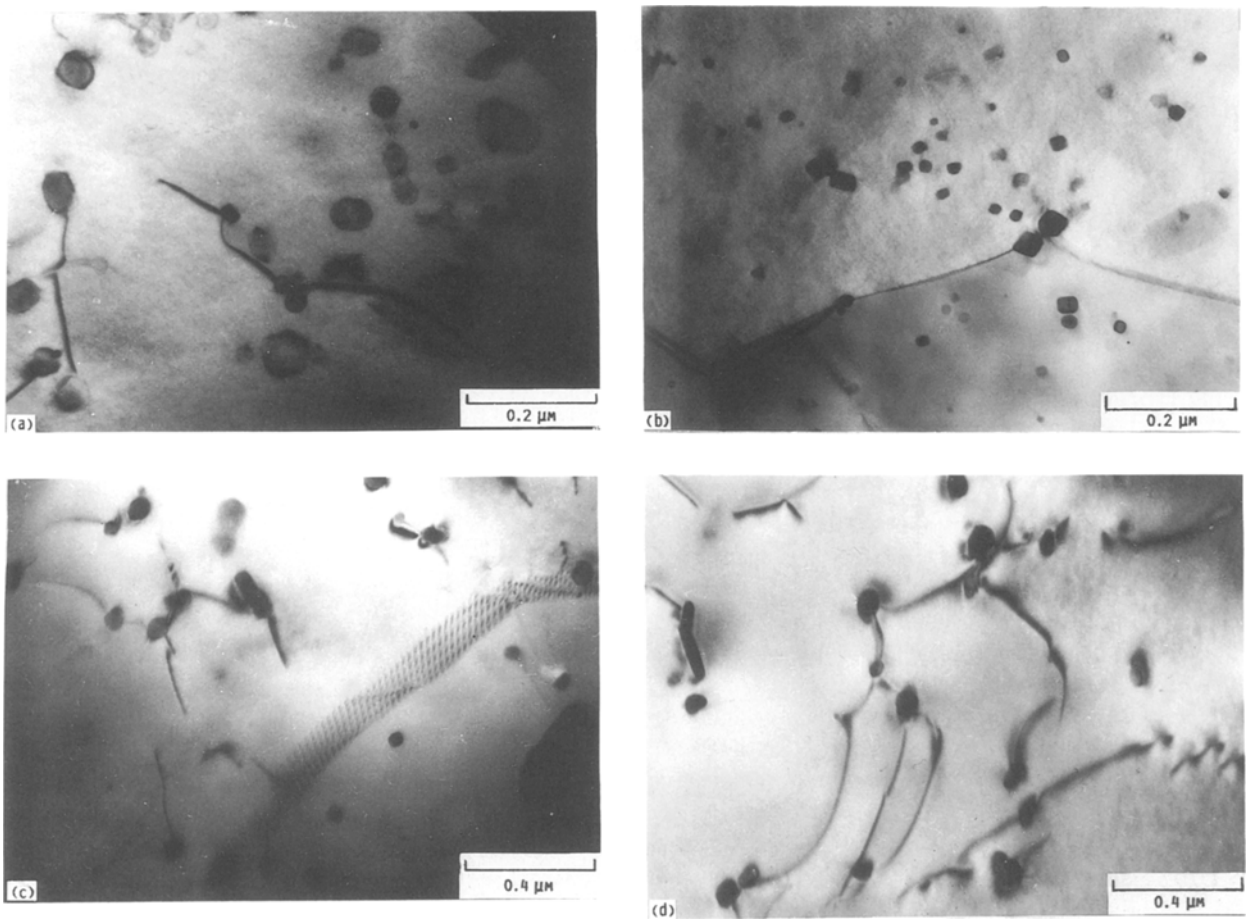

Figure 6 Transmission electron photomicrographs of RST dispersion strengthened NiAl specimens compression tested at 1300 K.

	Dispersoid	Approximate strain rate, (sec^{-1})	Flow stress at 5% strain, (MPa)	Final strain, (%)
(a)	$2TiB_2$	1.7×10^{-6}	30.4	8.0
(b)	2HfC	6.6×10^{-7}	63.0	13.0
(c)	4.3HfC	1.7×10^{-6}	62.5	9.5
(d)	4.3HfC	1.7×10^{-6}	62.5	9.5

4.3 HfC- containing intermetallics underwent secondary grain growth or recrystallization (Fig. 5b). Away from the large grain regions, a slight increase in the $\sim 2\,\mu m$ initial grain diameter was observed in these four materials. A similar degree of grain growth was found to uniformly take place in the NiAl–1 TiB_2, –1.5 TiB_2, –2 TiB_2 and –2 HfC dispersion strengthened alloys.

In view of the strength differences among the various RST dispersion strengthened intermetallics, TEM analysis was concentrated on the HfC-containing aluminides; however for comparative purposes one TiB_2-containing material was also examined. Figs 6a and b illustrate that the TiB_2 and HfC particles have remained small under elevated temperature deformation conditions, and these photomicrographs reinforce the previous observation that the size of the HfC dispersoid is significantly smaller and particle density is higher than those for TiB_2. While a mathematically meaningful study of dispersoid statistics was not undertaken, there appeared to be little difference in the distribution (size and density) of particles in the NiAl materials containing 1, 2 or 4.3% HfC. The ability of HfC to pin grain boundaries and act as potential anchors for subgrains is illustrated in Figs 6b and c respectively. Interactions between individual dislocations and the dispersoid are shown in Fig. 6a for TiB_2 and Fig. 6d for HfC. This latter photomicrograph is particularly interesting as it suggests that "departure side" pinning [12–14] of dislocations can occur in NiAl–HfC systems.

4. Discussion

From the TEM results (Fig. 2) it is clear that second phases can be dispersed as very small, on the order of 30 nm, diameter particles within a NiAl matrix through rapid solidification technology combined with hot extrusion as a densification procedure. Furthermore such dispersoids do possess some degree of thermodynamic stability as evidenced by the TEM photomicrographs of materials which experienced approximately 16 h (Figs 6a, c, and d) or 55 h (Fig. 6b) exposure at 1300 K during compression testing. However light optical and scanning electron microscopy study of certain materials ($2TiB_2$, 2 TiC or more than 0.5% HfC) indicates that distribution of the second phase is inhomogeneous as large precipitates can be found at random locations throughout

samples (Figs 1b and 5b). Although it is possible that such inhomogeneities are simply due to solubility limits for TiB_2, TiC and HfC in molten NiAl, extensive TEM analysis of a RST material needs to be undertaken to establish the uniformity or non-uniformity of the dispersion.

The mechanical property data (Figs 3 and 4) reveal that dispersions of HfC particles are effective elevated temperature hardening agents while neither TiB_2 or TiC dispersoids appear to be useful. This difference in strength due to dispersoid composition is unmistakably demonstrated by the comparison of the curves for the TiB_2 and TiC containing aluminides to that for NiAl–0.25 TiB_2–0.5 HfC in Fig. 4a. The lack of strengthening by TiB_2 is somewhat at odds with Jha *et al.* [7, 8] who reported that: (1) the 1033 K tensile strength of NiAl–TiB_2 was greater than that for NiAl; and (2) the strength increased with TiB_2 level for 0.25, 1.5 and 2TiB_2 containing materials. As decreasing the grain size improves the 1000 to 1400 K compressive properties [11], it is likely that the majority of stated strengthening is due to a grain size effect since their comparison pits nominally 2 μm intermetallics (Table I) against the $\sim 50\,\mu$m alloy of Rozner and Wasilewski [15]. Even with this in mind, however, it is difficult to understand Jha *et al.*'s dependency on TiB_2 content in view of the present data (Fig. 4a) where the 1.5 TiB_2 material is considerable weaker than either 0.25 or 2 TiB_2 levels.

If the RST manufactured aluminides are analogous to oxide dispersion strengthened (ODS) alloys, then the elevated temperature slow plastic strain rate properties of these materials should posses some indication of a threshold stress for creep. Typically evidence for such behaviour is reflected in high stress exponents; for example stress exponents ranging from 20 to 40 have been reported for TD–Ni [16], TD–NiCr [17] and MA 754 [18]. In the case of NiAl–HfC, high stress exponents are seen for the 0.5 HfC and 1 HfC intermetallics (Fig. 4b). Furthermore the independence of strain rate on stress for NiAl–2 HfC (Fig. 4b) as reflected by the poor fit (i.e. negligible coefficient of determination) of the power law equation is also indicative of a threshold stress. The data for NiAl–4.3 HfC also display a relatively mediocre fit; however the scatter in the stress–strain rate values is quite large. This might simply be a reflection on the current state of the art for RST processed dispersion strengthened aluminides. Most certainly as processing technology was being developed for ODS alloys, the elevated temperature mechanical properties of early heats of materials yielded inconsistent, but strong behaviour [19] similar to that shown for NiAl–2 HfC and –4.3 HfC in Fig. 4b.

Examination of the microstructure after testing (Table I, Fig. 5) reveals that extensive grain growth can occur. Such tendencies should be investigated in greater detail, particularly for as extruded materials. The need for this work stems from the observation [1, 11] that small grain size B2 crystal structure intermetallics are weaker than the large grain forms under very slow strain rate, extreme temperature conditions (for example 1300 K $-\ \dot{\varepsilon} < 10^{-7}\,\mathrm{sec}^{-1}$). Additionally research [17, 20–22] on ODS alloys has demonstrated the superior elevated temperature creep strength of highly elongated grain structures.

5. Summary

This study of NiAl-based composites containing TiB_2, TiC and HfC particles has indicated that rapid solidification technology is capable of producing dispersions of fine diameter particles within the intermetallic matrix; however only materials with HfC possessed elevated temperature strength exceeding that of binary NiAl. While there are strong suggestions of threshold stress behaviour in NiAl–HfC materials, examination of the microsctructure and the 1300 K stress–strain rate properties indicates that the distribution of dispersoids could be inhomogeneous and the as fabricated grain structures are not stable.

6. Conclusion

Rapid solidification technology is a viable method for the production of dispersion strengthened B2 crystal structure aluminides. However significant additional research is necessary to optimize the processing and development of this class of materials.

References

1. J. D. WHITTENBERGER, *J. Mater. Sci.* **22** (1987) 394.
2. K. VEDULA *et al.*, *Proc. MRS*, **39** (1985) pp. 411–21.
3. V. M. PATHARE, PhD Thesis, Case Western Reserve University, 1987.
4. R. K. VISWANADHAM *et al.*, High-Temperature/High Performance Composites, (*Proc. Mat. Res. Soc. Symp.*, **120**) edited by F. D. Lemkey, A. G. Evans, S. G. Fischman and J. R. Strife, (Pittsburgh, PA, 1988) pp. 94–99.
5. J. D. WHITTENBERGER *et al.*, *J. Mater. Sci.* **25** (1990) 35.
6. I. E. LOCCI *et al.*, "Microstructure, Properties and Processing of Melt Spun NiAl Alloys," presented at Fall '88 MRS Meeting, Boston, MA, 28 Nov-3 Dec 88.
7. S. C. JHA, R. RAY and P. CLEMM, "Fine Grain Nickel-Aluminide Alloy with Improved Toughness Made via Rapid Solidification Technology" Final report for contract NAS3-25132, July 1987.
8. S. C. JHA and R. RAY, *J. Mater. Sci. Lett.* **7** (1988) 285.
9. J. D. WHITTENBERGER, *Mater. Sci. Eng.* **57** (1983) 77.
10. *Idem., ibid.* **73** (1985) 87.
11. J. D. WHITTENBERGER, *J. Mater. Sci.* **23** (1988) 235.
12. V. C. NARDONE, D. E. MATEJCZYK and J. K. TIEN, *Acta Metall.* **32** (1984) 1509.
13. E. ARTZ and D. S. WILKINSON, *ibid.* **34** (1986) 1893.
14. E. ARTZ, J. RÖSLER and J. H. SCHRÖDER, "Creep and Fracture of Engineering Materials and Structures" (The Institute of Metals, London, 1987) p 217.
15. A. G. ROZNER and R. J. WASILEWSKI, *J. Inst. Met.* **94** (1966) 169.
16. B. A. WILCOX and A. H. CLAUER, *Trans. AIME* **236** (1966) 570.
17. B. A. WILCOX, A. H. CLAUER and W. S. McCAIN, *ibid.* **239** (1967) 570.
18. J. J. STEPHENS and W. D. NIX, *Met Trans.* **16A** (1985) 1307.
19. G. S. ANSELL and J. WEERTMAN, *Trans. AIME* **215** (1959) 838.
20. R. W. FRASER and D. J. I. EVANS, "Oxide Dispersion Strengthening", (Gordon and Breach, London 1968) p 375.
21. B. A. WILCOX and A. H. CLAUER, *Acta. Metall.* **20** (1972) 743.
22. J. D. WHITTENBERGER, *Met. Trans.* **8A** (1977) 1863.

Received 28 February
and accepted 30 August 1989